Distinct Meteorological Mode Associated with High-$PM_{2.5}$ Episodes in Seoul, South Korea

DANIEL CHOI,[a] HYO-JUNG LEE,[a,b] LIM-SEOK CHANG,[c] HYUN-YOUNG JO,[b] YU-JIN JO,[d] SHIN-YOUNG PARK,[e] GEUM-HEE YANG,[c] AND CHEOL-HEE KIM[a,b]

[a] *Department of Atmospheric Sciences, Pusan National University, Busan, South Korea*
[b] *Institute of Environmental Studies, Pusan National University, Busan, South Korea*
[c] *Environmental Satellite Center, National Institute of Environmental Research, Incheon, South Korea*
[d] *Department of Environmental Engineering Science, University of Florida, Gainesville, Florida*
[e] *Forecast Research Department, National Institute of Meteorological Sciences, Jeju, South Korea*

(Manuscript received 29 January 2023, in final form 27 April 2023, accepted 1 May 2023)

ABSTRACT: In this study, high–particulate matter ($PM_{2.5}$) pollution episodes were examined in Seoul, the capital city of South Korea, which, based on the episode characteristics, were influenced by a distinct meteorological mode, long-range transport (LRT), from two-level meteorological observations: surface and 850–500-hPa level. We performed two-step statistical analysis including principal component (PC) analysis of meteorological variables based on the observation data, followed by multiple linear regression (MLR). The meteorological variables included surface temperature (T_{sfc}), wind speed (WS_{sfc}), and the east–west (u_{sfc}) and north–south (v_{sfc}) components of wind speed, as well as wind components at 850-hPa geopotential height (u_{850} and v_{850}, respectively) and the vertical temperature gradient between 850 and 500 hPa. Our two-step analysis of data collected during the period 2018–19 revealed that the dominant factors influencing high-$PM_{2.5}$ days in Seoul (129 days) were upper-wind characteristics in winter, including positive u_{850} and negative v_{850}, that were controlled by the presence of continental anticyclones that increased the likelihood of LRT of $PM_{2.5}$ pollutants. Regional-scale meteorological variables, including surface and upper-meteorological variables on normal and high-$PM_{2.5}$ days, showed distinct covariation over Seoul, a megacity in the eastern part of northeast Asia with large anthropogenic emissions. Although this study examined only two atmospheric layers (surface and 500–850 hPa), our results clearly detected high-$PM_{2.5}$ episodes with LRT characteristics, suggesting the importance of considering both geographical distinctiveness and seasonal meteorological covariability when scaling down continental to local response to emission reduction.

KEYWORDS: Atmosphere; Asia; Air quality; Air pollution; Transportation meteorology

1. Introduction

Particulate matter (PM), particularly fine dust (diameter $<$ 10 μm; PM_{10}) and ultrafine particles (diameter $<$ 2.5 μm; $PM_{2.5}$), poses a serious threat to the atmospheric environment and human health (Franklin et al. 2008; Martins and da Graça 2018). High $PM_{2.5}$ pollutant levels in South Korea have led to the strengthening of government-mandated PM mitigation polices and emissions-reduction measures (J.-H. Kim et al. 2018; Park et al. 2020). In Korea, air quality including $PM_{2.5}$ is affected by synoptic meteorological conditions, as well as by the emission of both local primary pollutants and their gaseous precursors (Oh et al. 2015; Seo et al. 2017; Lee et al. 2019).

High-$PM_{2.5}$ episodes are the result of primary emission and secondary production via photochemical reactions. The chemical components of $PM_{2.5}$ are primary PM, secondary inorganic aerosols (SIAs) transformed from gaseous SO_2 and NO_x, organic carbon (OC) transformed from volatile organic compounds (VOCs), elemental carbon (EC), heavy metals, and mineral dust, among which SIAs such as SO_4^{2-}, NO_3^-, and NH_4^+ represent the largest component in northeast Asia (Hu et al. 2002; Andreae et al. 2008; Zhou et al. 2015; Yuan et al. 2022). Ammonium nitrate ($NH_3NO_3^-$) was recently found to be the main factor degrading air quality over numerous urban areas in northeast Asia. PM concentrations are additionally greatly influenced by emissions-control policies, synoptic- and local-scale meteorology, and physical and chemical processes.

Like several other megacities in northeast Asia, Seoul, South Korea, is facing increasingly high levels of $PM_{2.5}$. $PM_{2.5}$ is emitted from various sources including vehicles, roads and soil (as dust), combustion processes, industrial activities, and aerosols and their precursors; these emissions may be generated within an area or transported from outside, and further $PM_{2.5}$ is generated via chemical processes in the atmosphere (Ryou et al. 2018; Nam et al. 2018). Thus, the quantification of $PM_{2.5}$ is associated with considerable uncertainty due to its complex formation mechanisms. Several studies have attempted to assess the amount of $PM_{2.5}$ transported into Seoul using three-dimensional (3D) chemical transport models (Lee et al. 2022; Kim et al. 2017; Lee et al. 2017; Choi et al. 2019; National Institute of Environmental Research 2019). Nevertheless, it remains difficult to quantitatively

Choi's current affiliation: The Robert H. Smith Faculty of Agriculture, Food and Environment, Department of Soil and Water Sciences, The Hebrew University of Jerusalem, Rehovot, Israel.

Corresponding author: Cheol-Hee Kim, chkim2@pusan.ac.kr

DOI: 10.1175/JAMC-D-23-0016.1

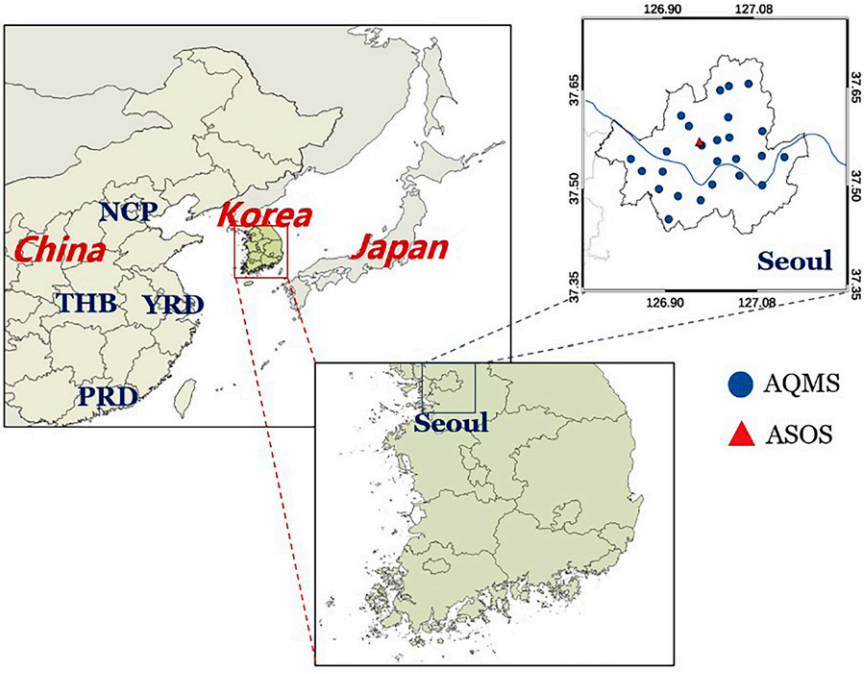

FIG. 1. Map of the study areas, indicating the locations of the PM measurement stations, Air Quality Monitoring Stations (AQMSs), and ASOS meteorological observation stations employed in this study. The North China Plain (NCP), Twin-Hu Basin (THB), Yangtze River Delta (YRD), and Pearl River Delta (PRD), which are high-emission source areas in northeastern Asia, are also indicated.

estimate the contributions of locally generated emissions and transported $PM_{2.5}$ due to several uncertainties including complicated meteorological factors.

Meteorological conditions have a particularly strong influence on short-term PM episodes through pollutant accumulation, regional transport, and secondary aerosol formation. Westerly winds also transport emitted pollutants to downwind urban areas at regional scales, indicating the importance of eastward medium-range transport in northeast Asia (Kaneyasu et al. 2014; Li et al. 2017; C.-H. Kim et al. 2018; Lee et al. 2022; Yoshino et al. 2021). Various statistical methods have been applied to study the meteorological factors influencing urban-scale air quality. For example, cluster analysis is used to classify wind patterns that impact PM concentrations (Kim et al. 2006; Lee et al. 2011; Jeon et al. 2019), and correlation analysis of PM concentration and meteorological variables is conducted to evaluate meteorological effects on PM concentrations (Galindo et al. 2011; Olvera-Alvarez et al. 2018; Dahari et al. 2020). Although correlation analyses are useful for understanding the linear contribution of each meteorological variable to PM concentration, these relationships are complicated by covariation among individual weather variables (Leung et al. 2018).

Principal component analysis (PCA) was developed by Obukhov (1947) as a multivariate statistical analysis technique (Wilks 2011); it has been applied for various purposes including the separation of spatial patterns among a range of a climatological variables (Lorenz 1956; Molteni et al. 1983; Björnsson and Venegas 1997), the identification of significant parameters in regression equations (Wahid et al. 2013), and dimension reduction for measurement data compression and inversion (Huang and Antonelli 2001). Tai et al. (2012) applied PCA to extract the meteorological modes influencing PM using various weather variables from assimilated meteorological data (GEOS-5) for the contiguous United States, and then conducted multiple linear regression (MLR) analysis to identify the dominant mode correlated with $PM_{2.5}$ variability. In addition to this conventional approach, Chang et al. (2021) applied PCA using data from surface observations and upper levels of the atmosphere to extract meteorological modes and then performed regression analysis of $PM_{2.5}$ concentrations in Seoul. Given the characteristics of high-$PM_{2.5}$ concentration episodes, it is important to analyze multilevel observations related to the accumulation, dissipation, and most importantly, long-range transport (LRT) of pollutants (Chang et al. 2021; Cai et al. 2017).

In this study, we investigated distinct meteorological modes promoting high-$PM_{2.5}$ episodes in Seoul. We performed PCA of meteorological variables based on both surface and 850-hPa observation data, followed by MLR to extract the dominant meteorological modes leading to high-$PM_{2.5}$ episodes. Because individual meteorological variables are covariant under a vertical synoptic system, this approach would lead to a more comprehensive understanding of the synoptic and mesoscale meteorological conditions that contribute to high-$PM_{2.5}$ episodes. The results of this study shed light on the

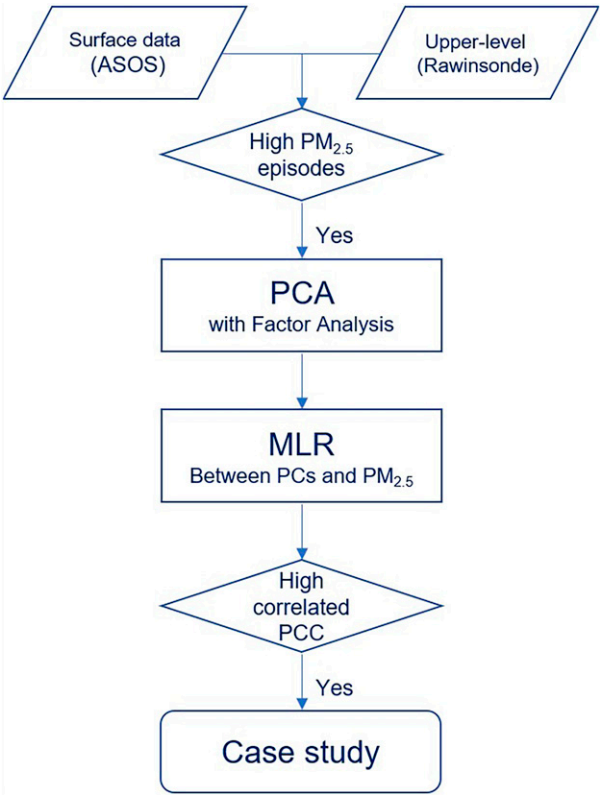

FIG. 2. Flowchart of our two-step statistical approach, which included PCA and MLR analysis. PCC indicates Pearson's correlation coefficient.

processes of $PM_{2.5}$ pollution and will lead to a more robust understanding of the mechanisms causing high-$PM_{2.5}$ episodes by analyzing observation data.

2. Methods and data

a. Study area

The current study targeted Seoul (37°33′N, 126°59′E), the megacity capital of South Korea (Fig. 1), which is located on the western Korean Peninsula. The Seoul metropolitan area (SMA) includes nearby satellite cities and has a population of 26.1 million. Recently, high $PM_{2.5}$ concentrations have persisted in the SMA for multiple days, creating an urgent pollution issue that has been addressed in studies of local emissions and long-range transboundary transport of air pollutants in the SMA (Jo and Kim 2013; Kim et al. 2012; Park et al. 2005, 2021). In 2015, annual emissions over the SMA included 50 603, 297 833, and 305 928 tons of PM_{10}, NO_x, and VOCs, respectively, among which PM_{10} and NO_x emissions were found to originate mainly from the traffic sector (National Institute of Environmental Research 2018).

b. Statistical analyses

In this study, we performed a two-step statistical analysis: PCA followed by MLR to extract the dominant meteorological modes associated with high-$PM_{2.5}$ episodes in Seoul based on meteorological observations collected at the surface and at 850 hPa. High-$PM_{2.5}$ days were defined as those with a daily average $PM_{2.5}$ level of $\geq 35\ \mu g\ m^{-3}$ in South Korea or with at least "bad" air quality on the South Korean forecasting scale ("good," "moderate," "bad," or "very bad"). To consider the synoptic meteorological time scale, we included the days before and after high-$PM_{2.5}$ days during the period 2018–19 for our two-step statistical analysis.

In our PCA analysis, the principal components (PCs) were linear combinations of meteorological variables from the surface and upper-level atmosphere; meteorological patterns (modes) represented by the factor loading of each weather variable were determined for high-PM concentration days. Next, MLR analysis of the PC modes and high-$PM_{2.5}$ daily mean concentrations was performed to obtain correlation coefficients (R values). Highly correlated PC modes were considered to characterize weather patterns occurring on high-$PM_{2.5}$ days. A flowchart of this two-step statistical approach is shown in Fig. 2.

We performed PCA by summing the PCs (U1, U2, U3, . . . , Un), each of which represents a linear combination of meteorological variables, X_k (Tai et al. 2012; Leung et al. 2018). Each PC was computed from the temporal mean $\overline{X_k}$ and

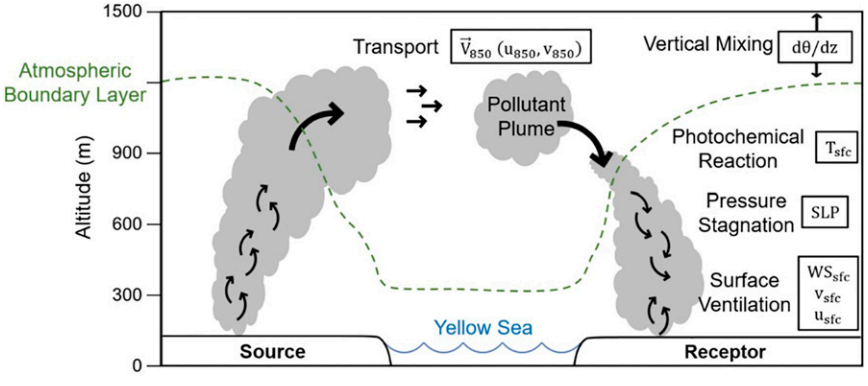

FIG. 3. Schematic diagram of $PM_{2.5}$ transport and distribution based on meteorological characteristics above and below the atmospheric boundary layer. See Table 1 for term definitions.

TABLE 1. Air pollutant data and meteorological variables used in this study. NIER is the National Institute of Environmental Research.

Variable	Description	Data source	Temporal resolution
	Atmospheric pollutants		
$PM_{2.5}$	Particulate matter with diameter <2.5 μm	NIER AQMS	1 h
	Surface meteorological variables		
T_{sfc}	Surface air temperature at 2 m (°C)	KMA ASOS	1 h
WS_{sfc}	Surface wind speed at 10 m (m s^{-1})	KMA ASOS	1 h
SLP	Sea level pressure (hPa)	KMA ASOS	1 h
u_{sfc}	West–east wind component at 10 m (m s^{-1})	KMA ASOS	1 h
v_{sfc}	South–north wind component at 10 m (m s^{-1})	KMA ASOS	1 h
	Meteorological variables at 850–500-hPa height		
u_{850}	West–east wind component at 850 hPa (m s^{-1})	KMA rawinsonde	12 h
v_{850}	South–north wind component at 850 hPa (m s^{-1})	KMA rawinsonde	12 h
$d\theta/dz$	Potential temperature difference between 850 and 500 hPa (K m^{-1})	KMA rawinsonde	12 h

standard deviation s_k of X_k, and the elements of the orthogonal transformation matrix $\boldsymbol{\alpha}_{kj}$, as follows:

$$U_j(t) = \sum_{k=1}^{n} \boldsymbol{\alpha}_{kj} \frac{X_k(t) - \overline{X_k}}{s_k}, \tag{1}$$

where each PC represents an individual meteorological mode; the modes were analyzed statistically according to the factor loading of each meteorological variable. In this study, daily $U_j(t)$ corresponding to weather patterns were investigated on high-$PM_{2.5}$ days to examine the generalized meteorological features of each PC.

Previous studies using similar approaches identified PCs that were strongly correlated with the $PM_{2.5}$ concentration as dominant meteorological modes influencing $PM_{2.5}$ variability (Tai et al. 2012; Chang et al. 2021). In a more generalized approach, we performed MLR analysis to compare correlations between the $PM_{2.5}$ concentration and each PC during high-$PM_{2.5}$ episodes, as follows:

$$\frac{Y(t) - \overline{Y}}{s_Y} = \sum_{j=1}^{n} \gamma_j U_j(t), \tag{2}$$

where Y is the regionally averaged $PM_{2.5}$ concentration, γ_j is a given PC regression coefficient, and $\overline{Y}$ and s_Y are the temporal mean and standard deviation of Y, respectively. Thus, in this study, meteorological PCs during high-$PM_{2.5}$ episodes were extracted through PCA, and the dominant horizontal weather patterns over the target domain during each high-$PM_{2.5}$ episode were determined through MLR analysis. This type of MLR analysis was described in greater detail by Tai et al. (2012) and Chang et al. (2021). This two-step analysis was performed using XLSTAT 2020 software (Addinsoft, New York, New York).

TABLE 2. Factor loadings for PCs during high-$PM_{2.5}$ episodes in Seoul, South Korea.

Variable	PC1	PC2	PC3	PC4	PC5	PC6	PC7	PC8
T_{sfc}	−0.89	0.21	−0.17	−0.07	0.01	−0.19	0.10	0.28
WS_{sfc}	0.28	0.81	−0.24	0.09	−0.19	0.25	−0.31	0.08
u_{sfc}	0.38	0.79	−0.12	0.02	0.17	0.00	0.42	−0.06
v_{sfc}	−0.58	0.23	0.49	0.26	0.51	0.17	−0.12	−0.01
SLP	0.78	−0.40	0.20	−0.06	0.09	0.32	0.14	0.22
u_{850}	0.46	0.24	0.68	0.34	−0.25	−0.30	−0.01	0.06
v_{850}	−0.73	−0.11	0.09	0.38	−0.39	0.31	0.22	−0.04
$d\theta/dz$	0.30	−0.27	−0.50	0.74	0.17	−0.11	−0.02	0.04

c. Observation data

We used hourly surface meteorological observation data collected by the Automated Surface Observing System (ASOS) and provided by the Korea Meteorological Administration (KMA; http://data.kma.go.kr). ASOS stations are distributed in 102 locations throughout South Korea (see Fig. 1) and are used to observe weather phenomena and share data through the Global Telecommunication System (GTS) of the World Meteorological Organization (WMO).

We also used rawinsonde upper-atmosphere observation data in this study. Rawinsonde provides information on non-surface atmospheric features by detecting upper-atmosphere temperature, humidity, pressure, and wind speed and direction data. The rawinsonde data had a coarser time resolution (12 h) than the surface observation data.

In this study, the surface data included temperature T_{sfc}, wind speed WS_{sfc}, and the east–west (u_{sfc}) and north–south (v_{sfc}) components of wind speed, as well as sea level pressure, whereas those observed at a geopotential height of 850 hPa included east–west and south–north wind speed components (u_{850} and v_{850}, respectively). $PM_{2.5}$ concentrations in South Korean megacities are influenced by external inflow from outer regions, which can be interpreted based on the geostrophic wind speed and direction at 500 or 850 hPa (Jo and Kim 2013; Kim et al. 2012; C.-H. Kim et al. 2018). For atmospheric stability, we calculated the vertical potential temperature gradient $d\theta/dz$ between two geopotential heights, which has previously been used for static stability. For example, Cai et al. (2017) used 850- and 500-hPa levels to construct a haze weather index, and Chang et al. (2021) used 850 and 500 hPa to quantify weather impacts on high $PM_{2.5}$ concentrations. Lee et al. (2022) simulated LRT over northeast Asia through limited

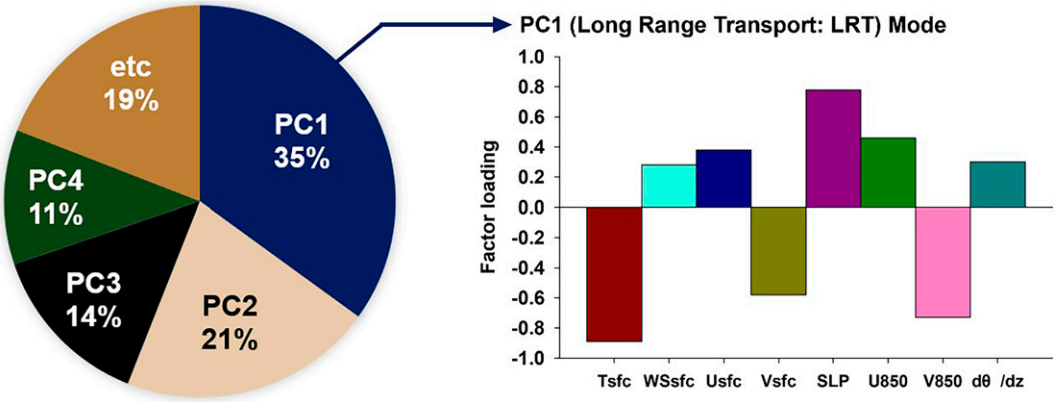

FIG. 4. The ratio of each PC and factor loadings for the dominant PC (PC1) during high-$PM_{2.5}$ episodes in Seoul.

layers ranging from 700 to 900 hPa, mainly above boundary layer height. Therefore, we selected heights of 850 and 500 hPa to calculate static stability. A schematic diagram of $PM_{2.5}$ evolution processes from a meteorological perspective is shown in Fig. 3. All meteorological variables are listed in Table 1. The data were collected during the period 2018–19, when $PM_{2.5}$ levels in Korean urban areas were unusually high.

3. Results and discussion

a. *Meteorological modes influencing the occurrence of high-$PM_{2.5}$ episodes*

The dominant PC (PC1) for 129 high-$PM_{2.5}$ days (>35 $\mu g\ m^{-3}$) in Seoul had factor loadings of −0.89, −0.58, 0.78, 0.46, and −0.73 for T_{sfc}, v_{sfc}, SLP, u_{850}, and v_{850}, respectively (Table 2, Fig. 4). PC1 accounted for 34.97% of the variation of all high-$PM_{2.5}$ days, with an eigenvalue of 2.80 (Table 3). The PCs were not correlated with temperature (factor loading of −0.89 for T_{sfc}) but were strongly correlated with east–west wind components at 850 hPa (factor loading of 0.46 for u_{850}) (Table 2 and Fig. 4). PC1 was much more highly significant in winter (Fig. 5).

PC2 was correlated with u_{sfc} and v_{sfc}; their increases indicated the arrival of southwesterly winds in Seoul, manifesting in haze formation over outer Seoul due to coastal point PM sources to the southwest or near the Yellow Sea, or to PM transport from sources in western or southern inland China such as the Yangtze River Delta, particularly during winter or spring. PC3 was correlated only with u_{850} in Seoul; its increase indicated synoptic strengthening of westerly winds, such that pollutants were transported from the North China Plain (NCP). We classified PC1–3 based on criteria described by Jo and Kim (2013); they distinguished LRT conditions by tracking consecutive 6-day synoptic weather charts and air trajectories and confirmed that PC1–3 represented LRT modes in Seoul.

Thus, weather patterns associated with PC1–3 frequently coincided with high-$PM_{2.5}$ episodes in Seoul, representing an important meteorological mode in this city. These patterns consist mainly of external contributions introduced by predominant westerly winds, suggesting that LRT processes from the western Korean Peninsula or external inflow promoted by westerly or northwesterly winds are the key meteorological modes for Seoul.

b. *High-$PM_{2.5}$ episodes associated with the dominant meteorological mode (PC1)*

We further examined the high-$PM_{2.5}$ episodes most influenced by PC1 attributes in Seoul, designated as cases 1, 3, and 4. In case 1 (22 March to 2 April 2018), the daily mean $PM_{2.5}$ concentration was 50.32 $\mu g\ m^{-3}$ (Table 4 and Fig. 6a), corresponding to a "very bad" grade among the four South Korean $PM_{2.5}$ forecast classes. MLR analysis showed that PC1 was most strongly correlated with $PM_{2.5}$ concentration among all PCs (R = 0.7) during this period. Surface and 850-hPa weather charts showed an anticyclone center located over the NCP (Fig. 7), which presumably transported pollutants via northwesterly winds (Fig. 7). We also examined the satellite-based aerosol optical depth (AOD) during this period, which also showed extremely high $PM_{2.5}$ concentrations over the target area (Fig. 8). Thus, PC1 was negatively correlated with temperature (Table 1 and Fig. 4), and the anticyclone centered over the NCP dominated northeast Asia, maintaining a pressure gradient force that generated northwesterly winds at 850 hPa that were conducive to downwind LRT of air pollutants from northeastern China toward Seoul

TABLE 3. Eigenvalue and variability explained by each PC during high-$PM_{2.5}$ episodes in Seoul.

PC	PC1	PC2	PC3	PC4	PC5	PC6	PC7	PC8
Eigenvalue	2.80	1.68	1.11	0.89	0.58	0.44	0.37	0.15
Variability (%)	34.97	21.01	13.83	11.10	7.21	5.44	4.59	1.85
Cumulative (%)	34.97	55.98	69.81	80.91	88.12	93.56	98.15	100.00

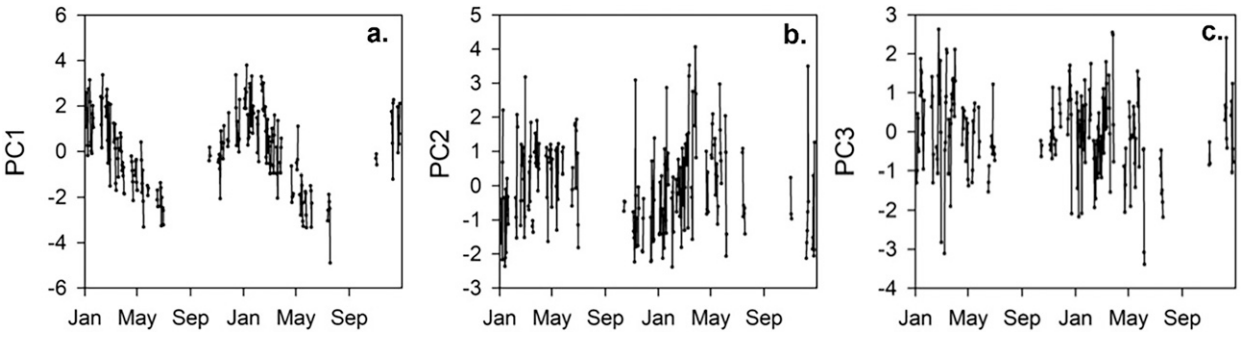

FIG. 5. Time series of PC1–3 for high-$PM_{2.5}$ episodes in Seoul.

(Fig. 7). This finding is consistent with reports by Jo and Kim (2013) and C.-H. Kim et al. (2018).

During case 3 (4–11 November 2018; mean $PM_{2.5}$ = 35.44 $\mu g\ m^{-3}$), $PM_{2.5}$ and PC1 were moderately correlated (R = 0.61), with a daily maximum $PM_{2.5}$ of 71.40 $\mu g\ m^{-3}$ on 6 November, followed by a decrease until 8 November and an increase until 10 November. This trend was highly consistent with the intensification of northwesterly winds (data not shown). During case 4 (20–27 February 2019; mean $PM_{2.5}$ = 48.87 $\mu g\ m^{-3}$), $PM_{2.5}$ and PC1 were again moderately correlated (R = 0.52), with a daily maximum $PM_{2.5}$ concentration of 62.17 $\mu g\ m^{-3}$ on 21 February. Thus, PC1 appears to be an important mode influencing high-$PM_{2.5}$-episode occurrence in Seoul. Synoptic weather charts during case 4 also indicated that PC1 was associated with enhanced $PM_{2.5}$ concentrations and that these conditions persisted until 25 February 2019 due to LRT processes characterized by northerly or northwesterly winds, with higher geostrophic wind speeds at 850 hPa ($|\mathbf{V}_g|$ = 8.7 m s^{-1}) over northeast Asia (Table 4); subsequently, $PM_{2.5}$ concentrations decreased as PC1 decreased.

c. *Distinct meteorological conditions associated with high $PM_{2.5}$*

Like several other megacities in northeast Asia, Seoul is also facing increasingly high levels of secondary air pollutants including $PM_{2.5}$ and O_3, which have become persistent issues (Lee et al. 2017; Choi et al. 2014; Kim et al. 2021; Oh et al. 2010; Lee et al. 2021). Studies on ambient secondary air pollutants have consistently reported their induction by transboundary transport into Seoul (Choi et al. 2014; Lee et al. 2019; Choi et al. 2019; Kim et al. 2021); however, comparing the estimated source contributions of local emissions and transported $PM_{2.5}$ remains challenging.

We examined observation-based meteorological factors to characterize high-$PM_{2.5}$ episodes in Seoul using a two-step PCA–MLR approach. Our statistically derived observation-based meteorological PCs yielded similar meteorological features to previous 3D chemical model estimates for Seoul, with differing seasonality. In Seoul, high-$PM_{2.5}$ episodes occurred mainly in winter and were correlated with external meteorological factors (Table 2). For example, as PC1 increased for Seoul, the temperature decreased and the SLP increased, perhaps due to continental anticyclones caused by the frequent northwesterly winds flowing into the Korean Peninsula (Fig. 7). PC2 indicated weaker seasonality, whereas PC3 indicated weak favoring of high-$PM_{2.5}$ episodes in winter. Interestingly, the atmospheric static stability ($d\theta/dz$) remained stable in Seoul under LRT conditions, mainly due to the presence of an anticyclone over northeast Asia (Table 2 and Fig. 4). However, it should be noted that the atmospheric static stability is the potential temperature gradient ($d\theta/dz$) between two levels (500 and 850 hPa), and should be distinguished from the

TABLE 4. Statistics for high-$PM_{2.5}$ episodes in Seoul obtained through PCA and MLR analysis.

High-$PM_{2.5}$ episode	Mean $PM_{2.5}$[a] ($\mu g\ m^{-3}$) and period	Daily max $PM_{2.5}$ ($\mu g\ m^{-3}$)	Date of max $PM_{2.5}$	Geostrophic wind speed[b] ($\lvert\mathbf{V}_g\rvert$) at 850 hPa (m s^{-1})	Corr-PC[c]	R[d]
Case 1	50.32 (22 Mar–2 Apr 2018)	98.91	25 Mar 2018	7.2	PC1	0.70
Case 2	39.92 (18–28 Feb 2018)	65.83	23 Feb 2018	12.3	PC3	0.66
Case 3	35.44 (4–11 Nov 2018)	71.40	6 Nov 2018	4.6	PC1	0.61
Case 4	48.87 (20–27 Feb 2019)	62.17	21 Feb 2019	8.7	PC1	0.52
Case 5	35.75 (10–18 May 2019)	45.44	15 May 2019	7.7	PC2	0.28

[a] Mean $PM_{2.5}$ concentrations during a high-$PM_{2.5}$ episode (duration in parentheses).
[b] $|\mathbf{V}_g| = (u_g^2 + v_g^2)^{1/2}$ was calculated by interpolating geostrophic wind components (u_g, v_g) at 37.5°N, 127.5°E, approximately the center of Korea, by using reanalysis data for four nearby grid points.
[c] One of five PCs that were highly correlated with the $PM_{2.5}$ concentration according to the MLR results.
[d] Here, R denotes Pearson's correlation coefficient.

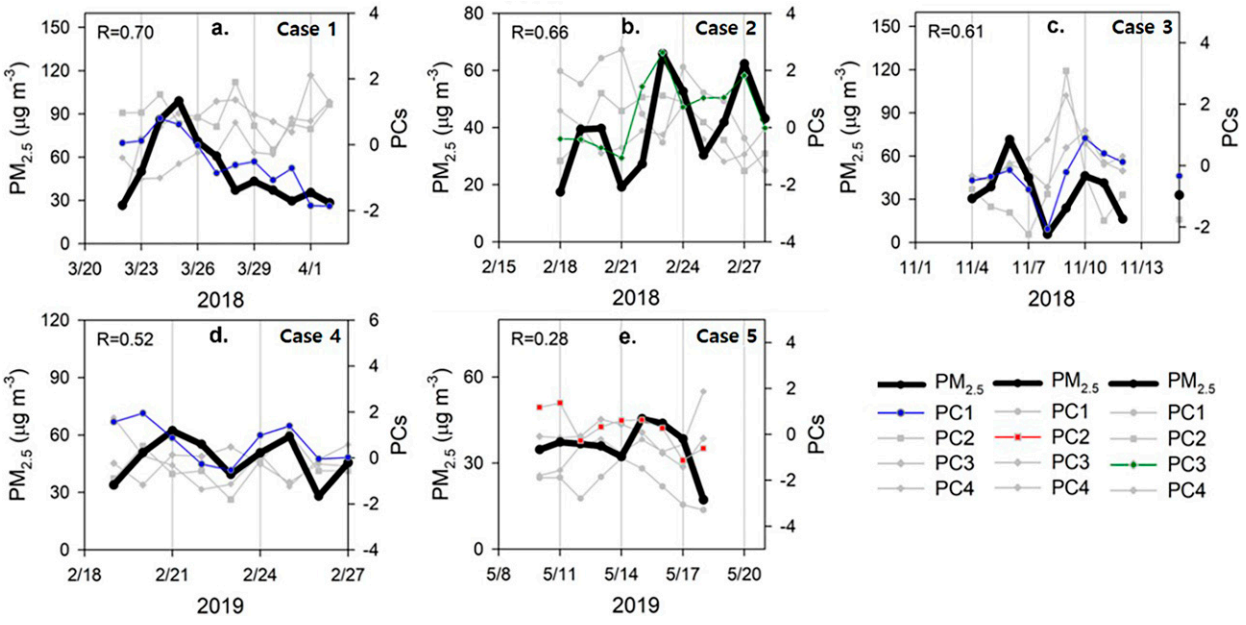

FIG. 6. $PM_{2.5}$ time series with each PC for five representative high-$PM_{2.5}$ concentration episodes (case 1–case 5).

vertical stability index of the lower atmosphere (S), which describes the temperature difference between the lower (T_1) and upper (T_2) levels ($S \equiv T_2 - T_1$), and is positive (stable) in stagnant meteorological conditions and negative (unstable) under LRT processes (Jo and Kim 2013). Overall, our results indicate a distinct meteorological mode with seasonality for high-$PM_{2.5}$ episodes in Seoul. Because this mode was associated with high $PM_{2.5}$ concentrations in our study, we infer that pollutants emitted from upstream areas, such as inland China, enhance pollution levels in air masses transported toward Seoul.

In summary, we analyzed high-$PM_{2.5}$ concentration days over Seoul, which were influenced by LRT processes; these episodes

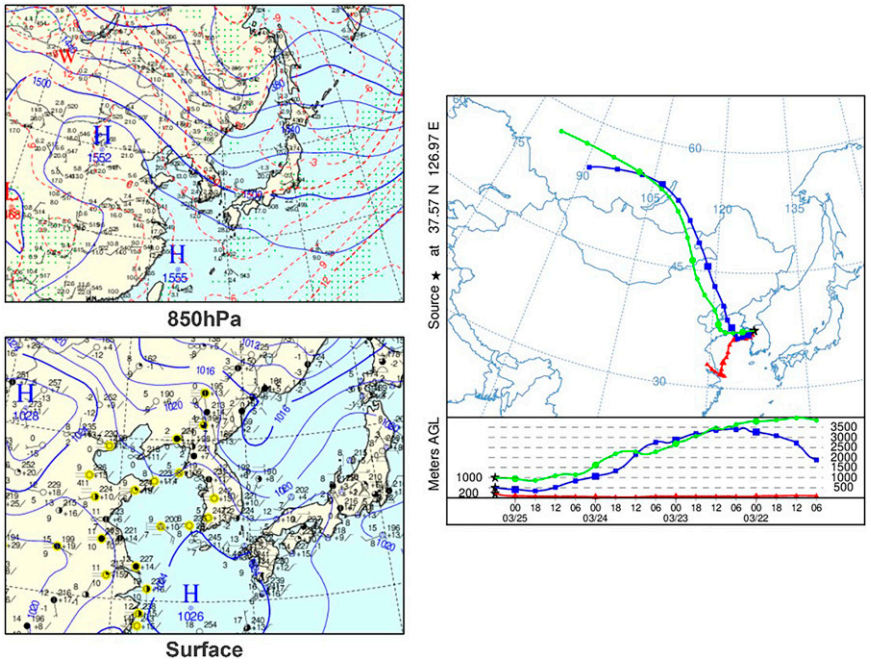

FIG. 7. (left) Synoptic weather maps at the (top) 850-hPa level and (bottom) surface produced by the KMA for 24 Mar 2018 (high-$PM_{2.5}$ case 1) and (right) a representative LRT case and backward trajectory of HYSPLIT model ending at 1500 LST 25 Mar 2018, with 96-h duration using GDAS meteorological data.

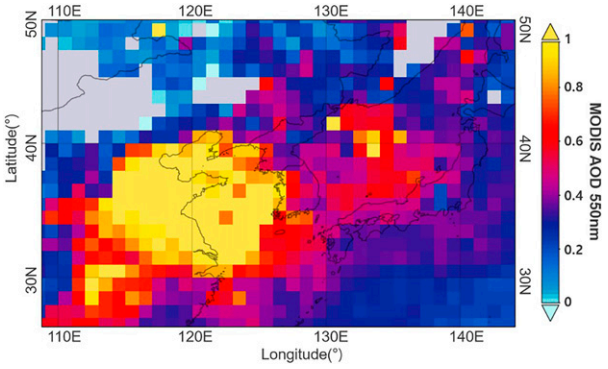

FIG. 8. Time-averaged spatial distribution of AOD 550 nm of MODIS *Aqua* during case1 from 22 Mar to 2 Apr 2018.

were associated with an anticyclone over Seoul. Based on the PC1 attributes, the frequency of high-$PM_{2.5}$ episodes in Seoul was greatly influenced by northwesterly winds at 850 hPa (Fig. 4). LRT processes were favored by relatively strong wind speed at the surface and at 850 hPa by air mass processes of pollutants under the prevailing high SLP system with a sinking upper atmosphere. The anticyclone that prevailed for the LRT cases favored the resultant northwesterlies, which transported pollutants emitted from central (or northern) China toward Seoul.

4. Conclusions

In this study, we performed a two-step statistical analysis consisting of PCA followed by MLR analysis using meteorological observations and $PM_{2.5}$ measurements as input data and interpreted the role of a dominant synoptic and mesoscale meteorological mode in high-$PM_{2.5}$ episodes in Seoul during the period 2018–19. First, we performed PCA to identify the meteorological characteristics during high-$PM_{2.5}$ episodes and calculated PCs, and then we conducted MLR analysis, from which a distinct mode was identified by analyzing correlations between the $PM_{2.5}$ concentration and PCA-derived meteorological PCs. The results showed that the dominant weather pattern associated with high-$PM_{2.5}$ episodes was related to LRT from the NCP to Seoul.

PC1 was the dominant mode, accounting for 35% of the variation observed for high-$PM_{2.5}$ episodes among all PCs; this PC was associated with decreased temperature, increased u, and decreased v at 850 hPa. Thus, the passage of an anticyclone (high SLP) over northeast Asia led to dominant northwesterly winds as indicated by increased PC1, in tandem with enhanced $PM_{2.5}$ concentrations in Seoul. These conditions were favorable for LRT of large amounts of $PM_{2.5}$, particularly in winter. MLR analysis also showed that high $PM_{2.5}$ concentrations were strongly associated with PC1. The dominant factors influencing high-$PM_{2.5}$ episodes in Seoul were associated with winter, including upper-atmosphere wind characteristics (positive u and negative v at 850 hPa), indicating the strong influence of winter continental anticyclones.

Our results also indicate that high-$PM_{2.5}$ episodes in South Korea exhibit strong seasonality, implying the necessity of season-dependent $PM_{2.5}$-reduction policies. This finding indicates the importance of both geographical distinctiveness over northeast Asia and seasonal meteorological covariation with high $PM_{2.5}$ in Seoul; therefore, international cooperation is critical to developing effective $PM_{2.5}$-mitigation strategies over northeast Asia. Further comprehensive studies employing 3D weather–air quality models that use reanalysis data, as well as more detailed $PM_{2.5}$ observations such as surface and upper-atmosphere chemical composition data and 3D remote sensing observations will allow us to better quantify $PM_{2.5}$ source contributions for the development of effective pollutant reduction strategies in large urban areas over northeast Asia.

Acknowledgments. This study was supported by the Basic Science Research Program through the National Research Foundation of Korea funded by the Ministry of Education of the Republic of Korea (Grants 2020R1I1A2075417 and 2020R1A6A1A03044834).

Data availability statement. Meteorological observation data are available from the Korea Meteorological Administration Weather Data Service. The $PM_{2.5}$ data are from Air Korea maintained by the Korea Environment Corporation.

REFERENCES

Andreae, M. O., O. Schmid, H. Yang, D. Chand, J. Z. Yu, L.-M. Zeng, and Y.-H. Zhang, 2008: Optical properties and chemical composition of the atmospheric aerosol in urban Guangzhou, China. *Atmos. Environ.*, **42**, 6335–6350, https://doi.org/10.1016/j.atmosenv.2008.01.030.

Björnsson, H., and S. A. Venegas, 1997: A manual for EOF and SVD analyses of climatic data. CCGCR Rep. 97-1, McGill University, 54 pp., https://muenchow.cms.udel.edu/classes/MAST811/eof.pdf.

Cai, W., K. Li, H. Liao, H. Wang, and L. Wu, 2017: Weather conditions conducive to Beijing severe haze more frequent under climate change. *Nat. Climate Change*, **7**, 257–262, https://doi.org/10.1038/nclimate3249.

Chang, L.-S., and Coauthors, 2021: Quantifying the impact of synoptic weather systems on high PM2.5 episodes in the Seoul metropolitan area, Korea. *J. Geophys. Res. Atmos.*, **126**, e2020JD034085, https://doi.org/10.1029/2020JD034085.

Choi, J., and Coauthors, 2019: Impacts of local vs. trans-boundary emissions from different sectors on $PM_{2.5}$ exposure in South Korea during the KORUS-AQ campaign. *Atmos. Environ.*, **203**, 196–205, https://doi.org/10.1016/j.atmosenv.2019.02.008.

Choi, K.-C., and Coauthors, 2014: Assessment of transboundary ozone contribution toward South Korea using multiple source–receptor modeling techniques. *Atmos. Environ.*, **92**, 118–129, https://doi.org/10.1016/j.atmosenv.2014.03.055.

Dahari, N., M. T. Latif, K. Muda, and N. Hussein, 2020: Influence of meteorological variables on suburban atmospheric $PM_{2.5}$ in the southern region of peninsular Malaysia. *Aerosol Air Qual. Res.*, **20**, 14–25, https://doi.org/10.4209/aaqr.2019.06.0313.

Franklin, M., P. Koutrakis, and P. Schwartz, 2008: The role of particle composition on the association between $PM_{2.5}$ and mortality. *Epidemiology*, **19**, 680–689, https://doi.org/10.1097/EDE.0b013e3181812bb7.

Galindo, N., M. Varea, J. Gil-Moltó, E. Yubero, and J. Nicolás, 2011: The influence of meteorology on particulate matter concentrations at an urban Mediterranean location. *Water Air Soil Pollut.*, **215**, 365–372, https://doi.org/10.1007/s11270-010-0484-z.

Hu, M., L.-Y. He, Y.-H. Zhang, M. Wang, Y. P. Kim, and K. C. Moon, 2002: Seasonal variation of ionic species in fine particles at Qingdao, China. *Atmos. Environ.*, **36**, 5853–5859, https://doi.org/10.1016/S1352-2310(02)00581-2.

Huang, H.-L., and P. Antonelli, 2001: Application of principal component analysis to high-resolution infrared measurement compression and retrieval. *J. Appl. Meteor. Climatol.*, **40**, 365–388, https://doi.org/10.1175/1520-0450(2001)040<0365:AOPCAT>2.0.CO;2.

Jeon, W., H. W. Lee, T.-J. Lee, J.-W. Yoo, J. Mun, S.-H. Lee, and Y. Choi, 2019: Impact of varying wind patterns on PM_{10} concentrations in the Seoul metropolitan area in South Korea from 2012 to 2016. *J. Appl. Meteor. Climatol.*, **58**, 2743–2754, https://doi.org/10.1175/JAMC-D-19-0102.1.

Jo, H.-Y., and C.-H. Kim, 2013: Identification of long-range transported haze phenomena and their meteorological features over northeast Asia. *J. Appl. Meteor. Climatol.*, **52**, 1318–1328, https://doi.org/10.1175/JAMC-D-11-0235.1.

Kaneyasu, N., and Coauthors, 2014: Impact of long-range transport of aerosols on the $PM_{2.5}$ composition at a major metropolitan area in the northern Kyushu area of Japan. *Atmos. Environ.*, **97**, 416–425, https://doi.org/10.1016/j.atmosenv.2014.01.029.

Kim, C.-H., S.-Y. Park, Y.-J. Kim, L.-S. Chang, S.-K. Song, Y.-S. Moon, and C.-K. Song, 2012: A numerical study on indicators of long-range transport potential for anthropogenic particulate matters over northeast Asia. *Atmos. Environ.*, **58**, 35–44, https://doi.org/10.1016/j.atmosenv.2011.11.002.

——, and Coauthors, 2018: Meteorological overview and signatures of long-range transport processes during the MAPS-Seoul 2015 campaign. *Aerosol Air Qual. Res.*, **18**, 2173–2184, https://doi.org/10.4209/aaqr.2017.10.0398.

——, and Coauthors, 2021: Comparative numerical study of $PM_{2.5}$ in exit-and-entrance areas associated with transboundary transport over China, Japan, and Korea. *Atmosphere*, **12**, 469, https://doi.org/10.3390/atmos12040469.

Kim, H. C., E. Kim, C. Bae, J. H. Cho, B.-U. Kim, and S. Kim, 2017: Regional contributions to particulate matter concentration in the Seoul metropolitan area, South Korea: Seasonal variation and sensitivity to meteorology and emissions inventory. *Atmos. Chem. Phys.*, **17**, 10 315–10 332, https://doi.org/10.5194/acp-17-10315-2017.

Kim, J.-H., H.-J. Kim, and S.-H. Yoo, 2018: Public value of enforcing the $PM_{2.5}$ concentration reduction policy in South Korean urban areas. *Sustainability*, **10**, 1144, https://doi.org/10.3390/su10041144.

Kim, Y.-K., S.-K. Song, H. W. Lee, C.-H. Kim, I.-B. Oh, Y.-S. Moon, and Z.-H. Shon, 2006: Characteristics of Asian dust transport based on synoptic meteorological analysis over Korea. *J. Air Waste Manage. Assoc.*, **56**, 306–316, https://doi.org/10.1080/10473289.2006.10464724.

Lee, H.-J., H.-Y. Jo, S.-Y. Park, Y.-J. Jo, W. Jeon, J.-Y. Ahn, and C.-H. Kim, 2019: A case study of the transport/transformation of air pollutants over the Yellow Sea during the MAPS 2015 campaign. *J. Geophys. Res. Atmos.*, **124**, 6532–6553, https://doi.org/10.1029/2018JD029751.

——, and Coauthors, 2021: Ozone continues to increase in East Asia despite decreasing NO_2: Causes and abatements. *Remote Sens.*, **13**, 2177, https://doi.org/10.3390/rs13112177.

——, and Coauthors, 2022: Transboundary aerosol transport process and its impact on aerosol-radiation-cloud feedbacks in springtime over northeast Asia. *Sci. Rep.*, **12**, 4870, https://doi.org/10.1038/s41598-022-08854-1.

Lee, H.-M., R. J. Park, D. K. Henze, S. Lee, C. Shim, H.-J. Shin, K.-J. Moon, and J.-H. Woo, 2017: $PM_{2.5}$ source attribution for Seoul in May from 2009 to 2013 using GEOS-Chem and its adjoint model. *Environ. Pollut.*, **221**, 377–384, https://doi.org/10.1016/j.envpol.2016.11.088.

Lee, K. J., S. B. Kim, and S.-K. Park, 2011: Daily, seasonal, and spatial patterns of PM_{10} in Seoul, Korea. *IEEE Int. Conf. on Intelligence and Security Informatics*, Beijing, China, Institute of Electrical and Electronics Engineers, 278–283, https://doi.org/10.1109/ISI.2011.5984097.

Leung, D. M., A. P. K. Tai, L. J. Mickley, J. M. Moch, A. van Donkelaar, L. Shen, and R. V. Martin, 2018: Synoptic meteorological modes of variability for fine particulate matter ($PM_{2.5}$) air quality in major metropolitan regions of China. *Atmos. Chem. Phys.*, **18**, 6733–6748, https://doi.org/10.5194/acp-18-6733-2018.

Li, T.-C., C.-S. Yuan, H.-C. Huang, C.-L. Lee, S.-P. Wu, and C. Tong, 2017: Clustered long-range transport routes and potential sources of $PM_{2.5}$ and their chemical characteristics around the Taiwan Strait. *Atmos. Environ.*, **148**, 152–166, https://doi.org/10.1016/j.atmosenv.2016.10.010.

Lorenz, E. N., 1956: Empirical orthogonal functions and statistical weather prediction. MIT Department of Meteorology Statistical Forecasting Project Scientific Rep. 1, 49 pp.

Martins, N. R., and G. C. da Graça, 2018: Impact of $PM_{2.5}$ in indoor urban environments: A review. *Sustainable Cities Soc.*, **42**, 259–275, https://doi.org/10.1016/j.scs.2018.07.011.

Molteni, F., P. Bonelli, and P. Bacci, 1983: Precipitation over northern Italy: A description by means of principal component analysis. *J. Climate Appl. Meteor.*, **22**, 1738–1752, https://doi.org/10.1175/1520-0450(1983)022<1738:PONIAD>2.0.CO;2.

Nam, J., S.-W. Kim, R. J. Park, J.-S. Park, and S. S. Park, 2018: Changes in column aerosol optical depth and ground-level particulate matter concentration over East Asia. *Air Qual. Atmos. Health*, **11**, 49–60, https://doi.org/10.1007/s11869-017-0517-5.

National Institute of Environmental Research, 2018: 2015 national air pollutants emission. https://www.air.go.kr/article/view.do?boardId=7&articleId=132&boardId=7&menuId=48&currentPageNo=1.

——, 2019: Summary report of the 4th stage (2013–2017). LTP Project Rep., 14 pp., https://www.me.go.kr/home/file/readDownloadFile.do?fileId=184686&fileSeq=1.

Obukhov, A. M., 1947: Statistically homogeneous fields on a sphere. *Usp. Mat. Nauk*, **2**, 196–198.

Oh, H.-R., C.-H. Ho, J. Kim, D. Chen, S. Lee, Y.-S. Choi, L.-S. Chang, and C.-K. Song, 2015: Long-range transport of air pollutants originating in China: A possible major cause of multi-day high-PM_{10} episodes during cold season in Seoul, Korea. *Atmos. Environ.*, **109**, 23–30, https://doi.org/10.1016/j.atmosenv.2015.03.005.

Oh, I.-B., Y.-K. Kim, M.-K. Hwang, C.-H. Kim, S. Kim, and S.-K. Song, 2010: Elevated ozone layers over the Seoul metropolitan region in Korea: Evidence for long-range ozone transport from eastern China and its contribution to surface concentrations. *J. Appl. Meteor. Climatol.*, **49**, 203–220, https://doi.org/10.1175/2009JAMC2213.1.

Olvera-Alvarez, H. A., O. B. Myers, M. Weigel, and R. X. Armijos, 2018: The value of using seasonality and meteorological variables to model intra-urban $PM_{2.5}$ variation. *Atmos. Environ.*, **182**, 1–8, https://doi.org/10.1016/j.atmosenv.2018.03.007.

Park, D.-H., S.-W. Kim, M.-H. Kim, H. Yeo, S. S. Park, T. Nishizawa, A. Shimizu, and C.-H. Kim, 2021: Impacts of local versus long-range transported aerosols on PM_{10} concentrations in Seoul, Korea: An estimate based on 11-year PM_{10} and lidar observations. *Sci. Total Environ.*, **750**, 141739, https://doi.org/10.1016/j.scitotenv.2020.141739.

Park, I.-S., W.-J. Choi, T.-Y. Lee, S.-J. Lee, J.-S. Han, and C.-H. Kim, 2005: Simulation of long-range transport of air pollutants over northeast Asia using a comprehensive acid deposition model. *Atmos. Environ.*, **39**, 4075–4085, https://doi.org/10.1016/j.atmosenv.2005.03.038.

Park, K., T. Yoon, C. Shim, E. Kang, Y. Hong, and Y. Lee, 2020: Beyond strict regulations to achieve environmental and economic health—An optimal $PM_{2.5}$ mitigation policy for Korea. *Int. J. Environ. Res. Public Health*, **17**, 5725, https://doi.org/10.3390/ijerph17165725.

Ryou, H. G., J. Heo, and S.-Y. Kim, 2018: Source apportionment of PM_{10} and $PM_{2.5}$ air pollution, and possible impacts of study characteristics in South Korea. *Environ. Pollut.*, **240**, 963–972, https://doi.org/10.1016/j.envpol.2018.03.066.

Seo, J., J. Y. Kim, D. Youn, J. Y. Lee, H. Kim, Y. B. Lim, Y. Kim, and H. C. Jin, 2017: On the multiday haze in the Asian continental outflow: The important role of synoptic conditions combined with regional and local sources. *Atmos. Chem. Phys.*, **17**, 9311–9332, https://doi.org/10.5194/acp-17-9311-2017.

Tai, A. P. K., L. J. Mickley, D. J. Jacob, E. M. Leibensperger, L. Zhang, J. A. Fisher, and H. O. T. Pye, 2012: Meteorological modes of variability for fine particulate matter ($PM_{2.5}$) air quality in the United States: Implications for $PM_{2.5}$ sensitivity to climate change. *Atmos. Chem. Phys.*, **12**, 3131–3145, https://doi.org/10.5194/acp-12-3131-2012.

Wahid, N. B., M. T. Latif, and S. Suratman, 2013: Composition and source apportionment of surfactants in atmospheric aerosols of urban and semi-urban areas in Malaysia. *Chemosphere*, **91**, 1508–1516, https://doi.org/10.1016/j.chemosphere.2012.12.029.

Wilks, D. S., 2011: *Statistical Methods in the Atmospheric Sciences*. 3rd ed. Elsevier, 676 pp.

Yoshino, A., A. Takami, K. Hara, C. Nishita-Hara, M. Hayashi, and N. Kaneyasu, 2021: Contribution of local and transboundary air pollution to the urban air quality of Fukuoka, Japan. *Atmosphere*, **12**, 431, https://doi.org/10.3390/atmos12040431.

Yuan, C.-S., K.-W. Wong, Y.-L. Tseng, J.-H. Ceng, C.-E. Lee, and C. Lin, 2022: Chemical significance and source apportionment of fine particles ($PM_{2.5}$) in an industrial port area in East Asia. *Atmos. Pollut. Res.*, **13**, 101349, https://doi.org/10.1016/j.apr.2022.101349.

Zhou, Y., S. Cheng, D. Chen, J. Lang, G. Wang, T. Xu, X. Wang, and S. Yao, 2015: Temporal and spatial characteristics of ambient air quality in Beijing, China. *Aerosol Air Qual. Res.*, **15**, 1868–1880, https://doi.org/10.4209/aaqr.2014.11.0306.